Title	Long term Aleutian Low dynamics and obliquity-controlled oceanic primary production in the mid-latitude western North Pacific (Core MD01-2421) during the last 145,000 years
Author(s)	Ueshima, Toshinori; Yamamoto, Masanobu; Irino, Tomohisa; Oba, Tadamichi; Minagawa, Masao; Narita, Hisashi; Murayama, Masafumi
Citation	Global and Planetary Change, 53(1-2), 21-28 https://doi.org/10.1016/j.gloplacha.2006.01.017
Issue Date	2006-08
Doc URL	http://hdl.handle.net/2115/14777
Type	article (author version)
File Information	G&PC53-1-2.pdf

Long term Aleutian Low dynamics and obliquity-controlled oceanic primary production in the mid-latitude western North Pacific (Core MD01-2421) during the last 145,000 years

Toshinori Ueshima[a], Masanobu Yamamoto[a,*], Tomohisa Irino[a], Tadamichi Oba[a], Masao Minagawa[a], Hisashi Narita[b] and Masafumi Murayama[c]

[a]*Graduate School of Environmental Earth Science, Hokkaido University, Kita-10, Nishi-5, Kita-ku, Sapporo 060-0810, Japan.*

[b]*School of Marine Science and Technology, Tokai University, 3-20-1, Orido, Shizuoka 424-8610, Japan.*

[c]*Center for Advanced Marine Core Research, Kochi University, 200 Mononobe, Nangoku, Kochi 783-8502, Japan.*

*Corresponding author: Phone/Fax: +81-11-706-2379, E-mail: myama@ees.hokudai.ac.jp (M. Yamamoto)

Abstract

We have generated an oceanic primary production record from Core MD01-2421, off central Japan, in the western North Pacific, for the last 145,000 years, in order to examine how the Aleutian Low has responded to orbital-scale climate change.

The variation of total organic carbon (TOC) was pronounced with a 41-kyr periodicity. High TOC corresponds to a high angle of the Earth's obliquity. The variation of TOC was delayed behind the variation of obliquity by ~1 kyr and preceded

the variation of $\delta^{18}O$ of benthic foraminifera *Uvigerina* by ~6 kyrs. The TOC varied inversely with Polar Circulation Index (Mayewski et al., 1997). Since the primary production in the Kuroshio-Oyashio mixed zone is related to the intensity of the winter Aleutian Low, these correspondences imply that the intensity of the winter Aleutian Low has responded to the obliquity forcing by the atmospheric reorganization in the northern high latitudes. The winter Aleutian Low was stronger when the obliquity was large, implying that the lower insolation in winter presumably increased the temperature contrast between the land and the ocean, deepening the winter Aleutian Low.

Keywords: primary production, organic carbon, the Aleutian Low, obliquity, IMAGES

1. Introduction

Reconstructing primary production (PP) can help us to understand the past changes of atmosphere-ocean dynamics. Enhanced PP is closely related to increased wind stress, as water mixing or upwelling causes the nutrient supply from the deeper ocean to the surface. The PP therefore is a good proxy for atmospheric circulation (e.g., Beaufort et al., 1997).

The primary production in the Kuroshio Extension region is sensitive to the intensity of the winter Aleutian Low (Goes et al., 2001). Although the production occurs mostly from spring to summer (Sawada et al., 1998), the primary production reflects the nutrient supply driven by the winter mixing of the ocean surface water, which is closely related to the Aleutian Low (Goes et al., 2001). During an El Niño year, PP was enhanced by the stronger winter Aleutian Low from spring to summer in the Kuroshio Extension region (Goes et al., 2001). The PP in this region, therefore, should reflect the past changes of the Aleutian Low.

The Aleutian Low is developed in winter in the northern North Pacific. The Aleutian Low is closely linked to the tropical El Niño-Southern Oscillation (ENSO) by the excitation of the Pacific and North America teleconnection pattern (Wallace and Gutzler, 1981). The decadal variation of the Aleutian Low is known as the Pacific Decadal Oscillation (Mantua et al., 1997), and it exerts a major influence on the winter climate of the north Pacific region and western North America (e.g., Mantua et al., 1997; Minobe, 1997). On a decadal time scale, the correlation between the Southern Oscillation Index and the Pacific Decadal Oscillation Index indicates the limited influence of tropical ENSO on the variation of the Aleutian Low (Dettinger et al., 2001). This observation suggests that the linkage between ENSO-like variability and the intensity of the Aleutian Low has not been constant on different time scales. On longer time scales, very little is known about the variations of the Aleutian Low and its linkage with the long-term ENSO-like variability (Clement et al., 1999; Beaufort et al., 2001; Yamamoto et al., 2004). Establishing the record of the Aleutian Low on orbital time scales will help us to understand the response of the Aleutian Low to glacial-interglacial climate change.

Yamamoto et al. (2004) showed a precession-controlled east-west seesaw-like change of alkenone SST in mid-latitude North Pacific margins, which was attributed mainly to the effect of orbital-scale changes in the ENSO behavior through atmospheric teleconnections. At the Japan margin (Core MD01-2421), the warmer periods, such as the MIS-2/3 and -3/4 boundaries, correspond to the periods when the tropical Pacific was in a La Niña-like condition, and the cooler periods, such as the MIS-1/2 and -5/6 boundaries, correspond to the periods when the tropical Pacific was in an El Niño-like condition. This correspondence suggested a strong linkage between the latitudinal displacement of the Kuroshio-Oyashio transition zone and the climatic condition of the tropical Pacific.

In this study, we have generated a primary production record from Core MD01-2421, off central Japan, for the last 145,000 years, in order to examine how the Aleutian Low has responded to orbital-scale climate change. The high sedimentation rate (average 33 cm/ky) of this core enabled us to achieve a high-resolution analysis.

2. Material and Method

A piston core MD01-2421 (45.82m long) was collected from off the coast of central Japan at 36°02’N, 141°47’E, and a 2224-meter water depth (Oba and KCRG, 2002) (Fig. 1). The sediments consist of homogeneous olive-gray silty clay with abundant siliceous and calcareous fossils. The age model was created by oxygen isotope stratigraphy (Martinson et al., 1987) of benthic foraminifera *Uvigerina* and *Bulimina aculeate*, by the C-14 derived calendar ages of 11 samples, and by the Aira-Tn ash layer at 28.59 ka (Murayama et al., 1993) (Fig, 2). The calendar ages were converted from the AMS C-14 ages of 11 samples of mixed planktonic foraminifera *Neogloboquadrina dutertrei* and *Globorotalia inflata* (0.31 to 43.33 ka) using the CALIB4.3 marine98 program (Stuiver and Reimer, 1993) and an equation of Bard (1998) with a 400-year global reservoir correction. This age model will be presented in more detail in Oba et al. (this special volume).

We obtained two different results for the linear sedimentation rate (LSR) in the interval of MIS-5 (Fig. 3). The LSR of case-I was obtained by the correlation of oxygen isotope profiles at both the mid-points and peaks in MIS-5. The LSR obtained in this way shows large fluctuations in MIS-5 (red line in Fig. 3). The LSR of case-II was obtained by the correlation of oxygen isotope profiles only at the mid-points. The LSR obtained in this way shows smaller variations than that of case-I (blue line in Fig. 3). Since there was no significant change in the sediment compositions in the interval of MIS-5 (Irino, unpublished data), we chose the result of case-II in this study.

Samples were freeze-dried and then crushed and milled to a particle size under 75μm. In all, 239 samples were analyzed with an average interval of 19 cm (610 years). Of these, 175 samples were analyzed for total organic carbon (TOC) using a LECO WR-112 carbon analyzer according to the method of Yamamoto (2003). The precision of measurement was better than 0.01 wt% (Yamamoto, 2003). The other 64 samples were analyzed for TOC, total nitrogen content (TN) and organic carbon isotope ratio ($\delta^{13}C$) using a Finnigan MAT 252 mass spectrometer connected to a Fisons NA 1500 elemental analyzer according to the method of Nakanishi and Minagawa (2003). Replicate errors in the analysis for an amino acid reagent were within ±0.2‰ for $\delta^{13}C$ (Nakanishi and Minagawa, 2003).

3. Results

Total organic carbon (TOC) content varied between 0.10 and 2.13 wt% of dry sediment, with an average of 1.18 wt% (Fig.3). The lowest TOC content was measured in a sandy sample (99 ka). Maximal peaks of TOC content were observed at 0-4 ka, 10-16 ka, 40-50 ka, 70-92 ka, 110 ka and 125-135 ka, whereas minimal values were observed at 20-30 ka, 60-70 ka, 102-112 ka and 122 ka.

The accumulation rate of organic carbon (OCAR) was obtained using the following equation:

$$OCAR\ (g/cm^2/kyr) = TOC\ (\%) \times DBD \times LSR/100$$

where DBD is dry bulk density (g/cm^3), and LSR is linear sedimentation rate (cm/ky). The LSR obtained in case-II was used for this calculation. OCAR varied between 0.03 and 0.56 $g/cm^2/kyr$, with an average of 0.26 $g/cm^2/kyr$ during 12-145 ka (Fig. 3). OCAR was not calculated in the Holocene interval, because sediment over-sampling was highly likely to occur with the Calypso corer (Széréméta et al., 2004). A comparison of the sediment weights of Core MD01-2421 with those of Core MD01-2420 and a gravity core KR02-06-St.A taken at the same site demonstrated an over-estimation of the mass accumulation rate in the uppermost 8 meters (Holocene interval) (Irino et al., 2004). The variation of OCAR was similar to that of the TOC content in MIS-2 to MIS-5d, while it differed from that of the TOC content in MIS-5e and MIS-6, because the profile was altered by the fluctuation of LSR (Fig. 3).

The weight ratio of total organic carbon to total nitrogen (C/N) varied between 7.5 and 9.7, with an average of 8.8 (Fig. 4). These values fell within the range typical of marine organic matter (4-10) (Meyers, 1994). C/N increased with increasing depth in the uppermost 9 meters (0-16 ka) of the core, which corresponds to the downward decreasing trend of TOC content over the same interval (Fig. 4). These phenomena are attributable to the early diagenetic degradation of labile organic matter. C/N has a good correlation with the $\delta^{13}C$ of organic matter ($r = -0.75$, $n = 64$, $p < 0.01$), indicating that both parameters reflect the relative contributions of terrestrial and marine organic matter in sediments.

The $\delta^{13}C$ of organic matter varied between -23.0 and -20.7‰, with an average of

-21.5‰ (Fig. 4). This range overlapped with and was slightly lighter than the range typical of marine organic matter (-22 ~ -20‰) (Meyers, 1994), indicating that the organic matter was derived mostly from marine organisms with a minor contribution of terrestrial C3 plants. The contents of terrestrial organic carbon (TROC%) and marine organic carbon (MROC%) in marine sediment can be estimated using the following equations:

$$\mathrm{TROC}\ (\%) = \{(\delta^{13}C_{marine} - \delta^{13}C_{sediment})/(\delta^{13}C_{marine} - \delta^{13}C_{terrestrial})\} \times \mathrm{TOC}$$

$$\mathrm{MROC}\ (\%) = \mathrm{TOC} - \mathrm{TROC}$$

where $\delta^{13}C_{marine}$ and $\delta^{13}C_{terrestrial}$ are the end-member values of carbon isotopic ratios of marine and terrestrial organic matters, respectively, and $\delta^{13}C_{sediment}$ is the value of a sediment sample.

We assumed the terrestrial and marine end-member $\delta^{13}C$ values to be -26.5‰ and -20.5‰, respectively, based on the results of case studies of the carbon isotopes of sedimentary organic matter in Tokyo Bay, in central Japan ($\delta^{13}C_{marine}$ = -21.5‰ to -20.1‰ and $\delta^{13}C_{terrestrial}$ = -26.5‰) (Wada et al., 1984), in Otsuchi Bay, in northeastern Japan ($\delta^{13}C_{marine}$ = -20.3‰ and $\delta^{13}C_{terrestrial}$ = -26.5‰) (Wada et al., 1990) and at the pelagic site of the NW Pacific ($\delta^{13}C_{marine}$ = -20.9 to -20.6‰) (Nakatsuka et al., 1997). The fraction of TROC ranged between 3% and 42% with an average of 17% (Fig. 4), which indicates that the organic matter in this core consisted mainly of marine organic matter, although some samples contained a significant amount of terrestrial organic matter. High TROC content was observed in the penultimate deglaciation period

(MIS-5/6 boundary) (Fig. 4).

TOC is often used as a paleo-indication of the sinking flux of organic matter in the water column to the sediment, but it is also influenced by changes in the dilution by clastics and/or the burial efficiency of organic matter with changing LSR, as reviewed in Tyson (1995). In MD01-2421, TOC content has a positive correlation with biogenic opal content ($r = 0.59$, $n = 139$, $p < 0.01$) and biogenic matter content (biogenic opal % + calcium carbonate % + 1.8 x TOC %) ($r = 0.62$, $n = 139$, $p < 0.01$) (Narita, unpublished data) and a negative correlation with detrital matter (100 % - total biogenic matter %), suggesting that the organic matter was associated with diatoms. OCAR has a positive correlation with biogenic opal AR ($r = 0.83$, $n = 124$, $p < 0.01$). Also, TOC content has a negative correlation with sand content ($r = 0.21$, $n = 136$, $p < 0.01$), and it has no significant correlation with silt ($r = 0.09$, $n = 136$) and clay contents ($r = 0.09$, $n = 136$) (Irino, unpublished data). These correlations imply that TOC content is independent of the influx of fine clastics, although it is affected by the dilution of biogenic matter by coarse clastics to some extent.

The burial efficiency of organic matter is also a factor influencing TOC content. Higher burial efficiency of organic matter in higher LSR results in higher TOC content (reviewed in Tyson, 1995). Nevertheless, TOC has little correlation with LSR ($r = 0.02$, $n = 236$) in MD01-2421, which indicates that the burial efficiency is not a major factor determining the TOC content in this core.

4. **Discussion**

Spectral analysis for TOC variation (the Blackman-Tuckey method with a bandwidth of 0.011) between 6 ka and 139 ka indicated a predominant 41-kyr periodicity, which corresponds to the change of the Earth's obliquity (Fig. 5). High TOC corresponds to a high angle of the Earth's obliquity. Cross-spectral analysis showed that the variation of TOC was delayed behind the variation of obliquity by ~1 kyr and preceded the variation of $\delta^{18}O$ of *Uvigerina* (Oba et al., submitted) by ~6 kyr.

The proxy records of the spring to summer SST from this core showed that the subarctic boundary in spring to early summer was displaced repeatedly with a precessional 23-kyr periodicity during the last 145 kyrs (Fig. 3; Yamamoto et al., 2004; Aizawa et al., 2004; Koizumi et al., 2004; Oba et al., submitted). Spectral analysis of alkenone SST indicated 23-kyr and 30-kyr periodicities rather than obliquity 41-kyr periodicity (Yamamoto et al., 2004). The 41-kyr periodicity observed in TOC variation was, therefore, not related to the latitudinal displacement of the subarctic boundary.

Modern oceanographic observations have suggested that the primary production in the Kuroshio-Oyashio mixed zone is related to the intensity of the winter Aleutian Low (Goes et al., 2001). Since the intensity of the winter Aleutian Low is high in El Niño events as a result of the excitation of the Pacific-North American teleconnection pattern (Wallace and Gutzler, 1981), the high primary production in the Kuroshio-Oyashio Extension region has often been linked to a tropical El Niño condition on an interannual time scale (Sugimoto et al., 2001; Goes et al., 2001).

Recent meteorological studies on a decadal timescale have shown the limited influence of tropical ENSO on the variation of the Aleutian Low (~25%), as indicated by the correlation between the Southern Oscillation Index and the Pacific Decadal Oscillation Index (r = -0.51; Dettinger et al., 2001). This observation suggests that the linkage between the ENSO-like variability and the Aleutian Low has not been constant on different time scales.

As to an orbital time scale, both a modeling study (Clement et al., 2001) and paleoceanographic evidence (Beaufort et al., 2001; Yamamoto et al., 2004) have suggested that the long-term ENSO-like variability became pronounced over 23-kyr (precession) and 30-kyr (unknown) cycles rather than a 41-kyr (obliquity) cycle. These findings suggest that the variation of the Aleutian Low that varied with the obliquity 41-kyr cycle may have been almost independent of the tropical climatic forcing.

Both the predominant 41-kyr and 23-kyr cycles were found in TOC and SST records, respectively, from the same core (Fig. 3). This phenomenon is attributed to difference in the season that was recorded by each proxies. The alkenone SST recorded the early summer SST, because the alkenones are produced mainly in early summer in this region (Sawada et al., 1998). The TOC reflects the nutrient supply by surface water mixing in winter (Goes et al., 2001). This core, therefore, recorded both the precession-controlled summer climatic phenomena and the obliquity-controlled winter phenomena.

The short time-lag (~1 kyr) between the variations of obliquity and TOC (Fig. 3) suggests that the intensity of the winter Aleutian Low has responded to the orbital forcing by changes in atmospheric-ocean interactions rather than by changes in the ice sheets of the northern hemisphere. In fact, the TOC variation is reverse of that of the polar circulation index (PCI), which provides a relative measure of the average size and intensity of polar atmospheric circulation, recorded in the Greenland ice core (Mayewski et al., 1997); High TOC correlates with low PCI, and vice verse (Fig. 3). This correlation implies that when the Aleutian Low was weaker, more continental dusts and marine chemical species were transported to central Greenland, and vice verse, suggesting that the TOC variation reflects the atmospheric reorganization in the northern high latitudes.

The winter Aleutian Low was stronger when the obliquity was large, implying that the lower insolation in winter presumably increased the temperature contrast between the land and the ocean, deepening the winter Aleutian Low. Modern oceanographic observations demonstrated that the stronger Aleutian Low increases the flow of the Kuroshio Current (Kawabe, 2001). This relationship implies that the enhanced flow of the Kuroshio increases the heat flow to the subarctic gyre of the North Pacific and further deepens the winter Aleutian Low. This positive feedback mechanism in the atmosphere-ocean interaction might be a potential amplifier of the orbital forcing.

This study demonstrated the orbital-scale variation of TOC in the mid-latitude northwestern Pacific, which we attributed to changes in the Aleutian Low that occur with the obliquity 41-kyr cycle. The Aleutian Low was stronger at the glacial terminations, suggesting that the variation of the Aleutian Low was linked to global warming in the deglaciation period, although we do not know whether the variation of Aleutian Low is a forcing or response of climate change. Further studies are indispensable in this regard for a better understanding of the response of the variation of the Aleutian Low to glacial-interglacial climate change and its role in global warming at deglaciations.

5. Conclusions

This study demonstrated that the variation of TOC in the mid-latitude northwestern Pacific varied synchronously with the change of the Earth's obliquity and inversely with the concentrations of continental dusts and marine chemical species in a Greenland ice cores, suggesting that the intensity of the winter Aleutian Low has responded to the obliquity forcing by the atmospheric reorganization in the northern high latitudes. The winter Aleutian Low was stronger when the obliquity was large, implying that the lower insolation in winter presumably increased the temperature contrast between the land and the ocean, deepening the winter Aleutian Low. The intensity of the Aleutian Low that varied with the obliquity 41-kyr cycle may have been almost independent of the tropical climate that varied with precession 23-kyr cycle.

Acknowledgements

We would like to thank N. Edasawa and T. Kuramoto for their analytical assistance in isotopic measurements. In addition, we are grateful to H. Kawahata, S. Minobe, K. Yamazaki and the members of the Kashima Core Research Group for their discussions of this topic. Comments by Luc Beaufort, Anne Mueller, Yair Rosenthal improved this manuscript. This study was supported by grants-in-aid for Scientific Research of JSPS, No 13304040 and GCMAPS of MEXT.

References

Aizawa, C., Oba, T, Okada, H., 2004. Late Quaternary paleoceanography deduced from coccolith assemblage in a piston core recovered from off coast of central Japan. Mar. Micropaleontol. 52, 277-297.

Bard, E., 1998. Geochemical and geophysical implications of radiocarbon calibration. Geochim. Cosmochim. Acta 62, 2025-2038.

Beaufort, L., de Garidel-Thoron, T., Mix, A.C., Pisias, N.G., 2001. ENSO-like forcing on oceanic primary production during the late Pleistocene. Science 293, 2440-2444.

Clement, A.C., Seager, R., Cane, M.A., 1999. Orbital controls on the El Niño/Southern

Oscillation and the tropical climate. Paleoceanogr. 14, 441-456.

Dettinger, M.D., Battisti, D.S., Garreaud, R.D., McCabe, Jr., G.J., Bitz, C.M., 2001. Interhemispheric effects of interannual and decadal ENSO-like climate variations on the Americas. In: Markgraf, V. (ed.), Interhemispheric Climate Linkages. Academic Press, San Diego, pp. 1-16.

Goes, J.I., Gomes, H.R., Limsakul, A., Balch, W.M., Saino, T., 2001. El Niño related interannual variations in biological production in the North Pacific as evidenced by satellite and ship data. Prog. Oceanogr. 49, 211-225.

Irino, T., Sagawa, T., Ikehara, K., Oba, T., Kawahata, H., 2004. Difference in coretop weight among three sediment cores recovered from off-Kashima, Japan. JAMSTEC J. Deep Sea Res. 24, 79-83. (in Japanese, with English abstr.)

Kawabe, M., 2001. Interannual variations of sea level at the Nansei Islands and volume transport of the Kuroshio due to wind changes. J. Oceanogr. 57, 189-205.

Koizumi, I., Irino, T., Oba, T., 2004. Paleoceanography off central Japan based on diatom flora during the latest Quaternary. Mar. Micropaleontol. 53, 293-365.

Martinson, D.G., Pisias, N.G., Hays, J.D., Imbrie, J., Moore, Jr., T.C., Shackleton, N.J., 1987. Age dating and the orbital theory of the ice ages: Development of a high-resolution 0 to 300,000-year chronostratigraphy. Quat. Res. 27, 1-29.

Mantua, N.J., Hare, S.R., Zhang, Y., Wallace, J.M., Francis, R.C., 1997. A Pacific interdecadal climate oscillation with impacts on salmon production. Bull. Amer. Meteor. Soc. 78, 1069-1079.

Mayewski, P.A., Meekerm, L.D., Whitelow, S., Twickler, M.S., Morrison, M.C., Bloomfield, P., Bond, G.C., Alley, R.B., Gow, A.J., Grootes, P.M., Meese, D.A., Ram, M., Taylor, K.C., Wumkes, W., 1994. Changes in atmospheric circulation and ocean ice cover over the North Atlantic during the last 41,000 years. Science 263, 1747-1751.

Meyers, P.A., 1994. Preservation of elemental and isotopic source identification of sedimentary organic matter. Chem. Geol. 114, 289-302.

Minobe, S., 1997. A 50-70 year climate oscillation over the North Pacific and North America. Geophys. Res. Let. 24, 683-686.

Mizuno, K., White, W.B., 1983. Annual and interannual variability in the Kuroshio Current System. J. Physiol. Oceanogr. 13, 1847-1867.

Murayama, M., Matsumoto, E., Nakamura, T., Okamura, M., Yasuda H., Taira, A., 1993. Re-examination of the eruption age of Aira-Tn Ash (AT) obtained from a piston core off Shikoku. J. Geol. Soc. Japan 99, 787-798.

Nakanishi, T., Minagawa, M., 2003. Stable carbon and nitrogen isotopic compositions of sinking particles in the northeast Japan Sea. Geochem. J. 37, 261-275.

Nakatsuka, T., Handa, N., Harada, N., Sugimoto, T., Imaizumi, S., 1997. Origin and decomposition of sinking particle organic matter in the deep water column inferred from the vertical distributions of its $\delta^{15}N$, $\delta^{13}C$ and $\Delta^{14}C$. Deep-Sea Res, 44, 1957-1979.

Oba, T., Kashima Core Research Group, 2002. Multi-disciplinary analysis of IMAGES core (MD012421) in the northwest Pacific Ocean. paper presented at AGU 2002 Fall Meeting, San Francisco, 6-10 December, 2002.

Oba, T., Irino, T., Yamamoto, M., Murayama, M., Takamura, A., Aoki, K., Paleoceanographic change off central Japan since the last 145,000 years based on high-resolution oxygen and carbon isotope records. Submitted to Global and Planetary Change, this special volume.

Sawada, K., Handa, N., Nakatsuka T, 1998. Production and transport of long-chain alkenones and alkyl alkenoates in a sea water column in the northwestern Pacific off central Japan. Mar. Chem. 59, 219-234.

Stuiver, M., Reimer, P., 1993. Extended ^{14}C database and revised CALIB 3.0 ^{14}C age model calibration program. Radiocarbon 35, 215-230.

Sugimoto, T., Kimura, S., Tadokoro, K., 2001. Impact of El Niño events and climate regime shift on living resources in the western North Pacific. Prog. Oceanogr. 49, 113-127.

Széréméta, N., Bassinot, F., Balut, Y., Labeyrie, L., Pagel, M., 2004. Oversampling of sedimentary series collected by giant piston corer: Evidence and corrections based on 3.5-kHz chirp profile. Paleoceanogr. 19, PA1005, doi: 10.1029/2002PA000795.

Tyson, R. V., 1995. Sedimentary Organic Matter – Organic Facies and Palynofacies. Chapman & Hall, London.

Wada, E., Mizutani, H., Karasawa, K., Kobayashi, Y., Minagawa, M., Yomemoto, T., 1984. Carbon and nitrogen composition as tracers of transport of organic matter along the Otsuchi watershed. Chikyu-kagaku 18, 89-98. (in Japanese)

Wada, E., Kabaya, Y., Tsuru, K., Ishiwatari, R., 1990. ^{13}C and ^{15}N abundance of sedimentary organic matter in estuarine areas of Tokyo Bay, Japan. Shitsuryo Bunseki (Mass Spectrosc.) 38, 307-318. (in Japanese, with English abstr.)

Wallace, J.M., Gutzler, D.S., 1981. Teleconnections in the geopotential hight field during the Northern Hemisphere winter. Mon. Wea. Rev., 109, 784-812.

Yamamoto, M., 2003. Data Report: Organic carbon, and alkenone sea-surface temperature from Sites 1175, 1176, and 1178, Nankai Trough. Proc. ODP, Sci. Res., 190, 196, 1-10.

Yamamoto, M., Oba, T., Shimamune J., Ueshima, T., 2004. Orbital-scale anti-phase variation of sea surface temperature in mid-latitude North Pacific margins during the last 145,000 years. Geophys. Res. Let., 31, L16311, doi:10.1029/2004GL020138.

Figure captions

Fig. 1. Location of site IMAGES MD01-2421 (36°02'N, 141°47'E, 2224 meters deep) and the Kuroshio and Oyashio currents (Mizuno and White, 1983).

Fig. 2. Age depth models of Core MD01-2421 (Oba et al., submitted).

Fig. 3. Changes in linear sedimentation rate (LSR; red line: case-I; blue line: case-II), total organic carbon content (TOC), organic carbon accumulation rate (OCAR), $\delta^{18}O$ of benthic foraminifera (blue: *Uvigerina*; green: *Bulimina* [+0.11 permil]; Oba et al., submitted), $U^{K'}_{37}$-based sea surface temperature (SST) (Yamamoto et al., 2004), calculated NINO3 index (Clement et al., 1999) and the Polar Circulation Index (PCI; Mayewski et al., 1997) during the last 145,000 years. The 41-kyr-filtered TOC variation (green) and the change of obliquity (red) were also shown in the figure.

Fig. 4. Changes in organic carbon isotope composition ($\delta^{13}C$), the weight ratio of total organic carbon to total nitrogen (C/N), terrestrial organic carbon content (TROC%), marine organic carbon content (MROC%) and the fraction of TROC in TOC (TROC % of TOC) during the last 145,000 years.

Fig. 5. Spectral densities and coherencies of TOC versus obliquity and the $\delta^{18}O$ of

benthic foraminifera *Uvigerina* (6.0-139.8 ka, bandwidth = 0.011).

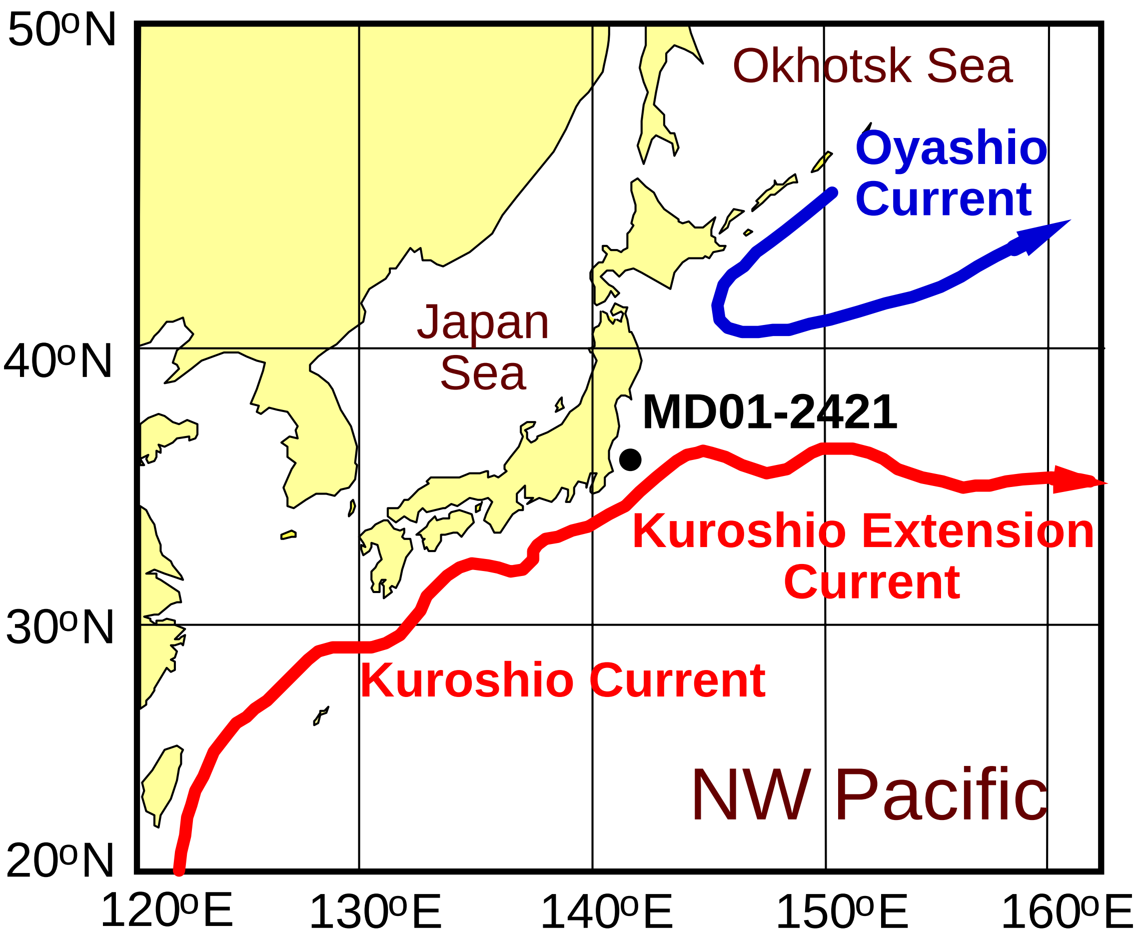

Fig. 1

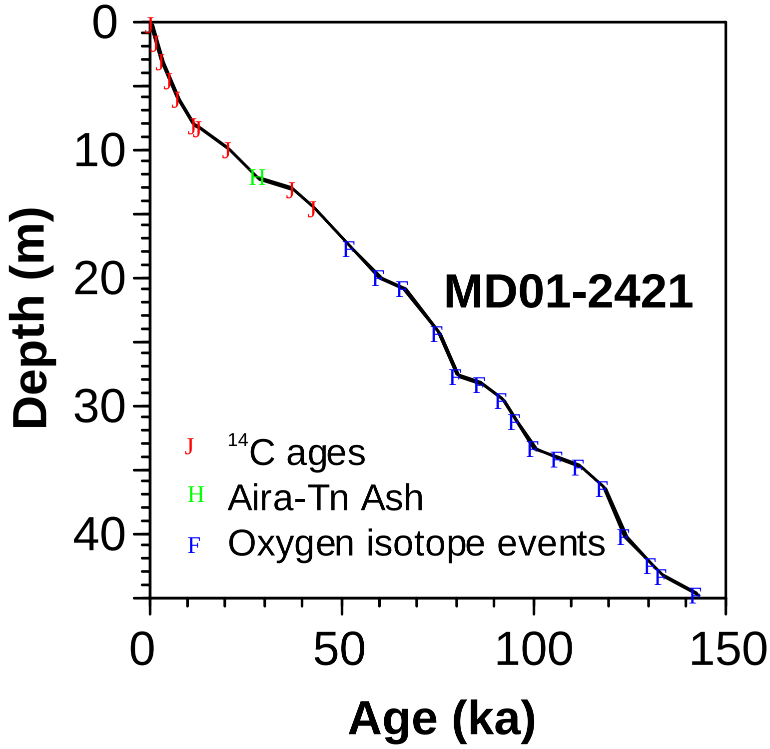

MD01-2421
Depth (m)
Age (ka)
0
10
20
30
40
0
50
100
150
14C ages
Aira-Tn Ash
Oxygen isotope events

Fig. 2

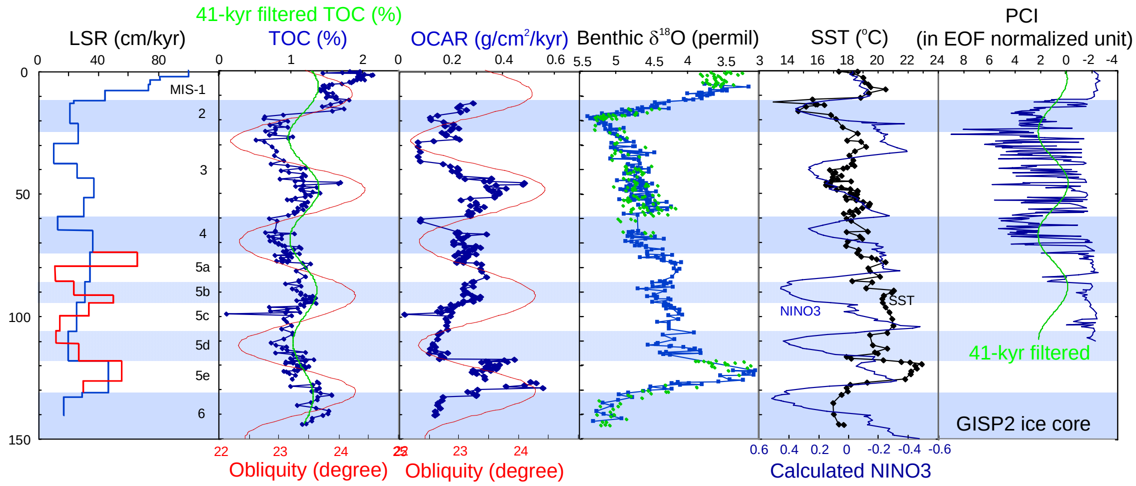
LSR (cm/kyr)
41-kyr filtered TOC (%)
TOC (%)
OCAR (g/cm2/kyr)
Benthic δ18O (permil)
SST (°C)
PCI
(in EOF normalized unit)
MIS-1
2
3
4
5a
5b
5c
5d
5e
6
NINO3
SST
41-kyr filtered
GISP2 ice core
Obliquity (degree)
Obliquity (degree)
Calculated NINO3

Fig. 3

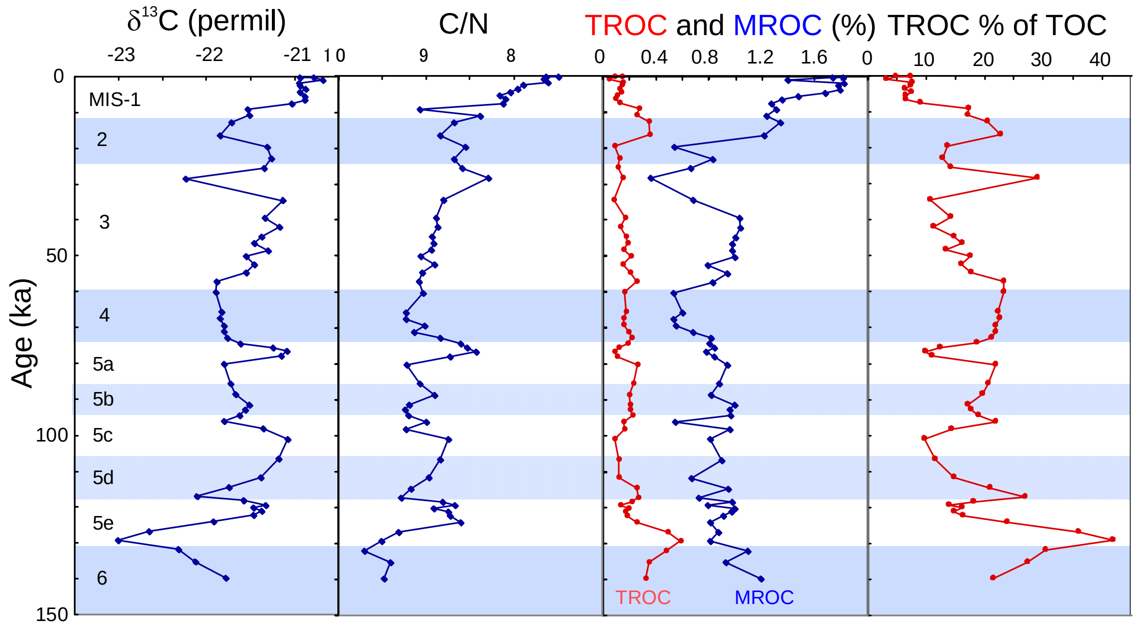

δ13C (permil)
-23
-22
-21
C/N
10
9
8
TROC and MROC (%)
0
0.4
0.8
1.2
1.6
TROC % of TOC
0
10
20
30
40
Age (ka)
0
50
100
150
MIS-1
2
3
4
5a
5b
5c
5d
5e
6
TROC
MROC

Fig. 4

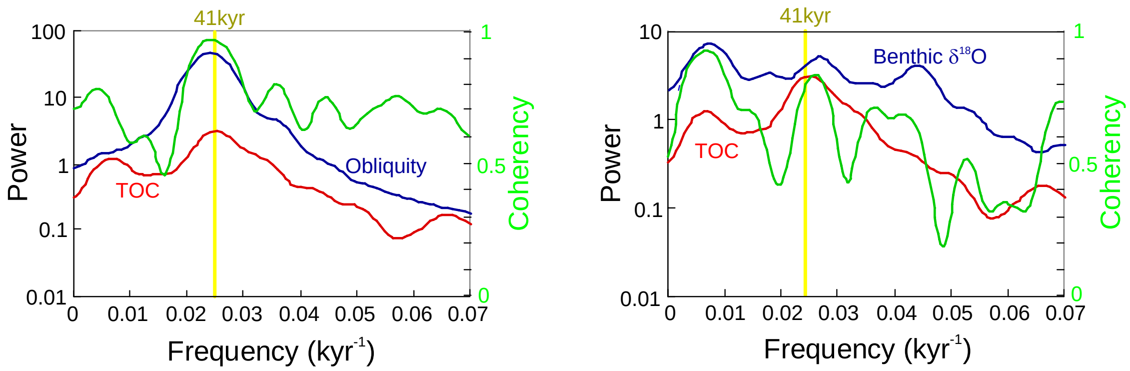
41kyr
100
10
1
0.1
0.01
Power
TOC
Obliquity
1
0.5
0
Coherency
0
0.01
0.02
0.03
0.04
0.05
0.06
0.07
Frequency (kyr-1)
41kyr
10
1
0.1
0.01
Power
TOC
Benthic δ18O
1
0.5
0
Coherency
Frequency (kyr-1)

Fig. 5